

Incorporation of ferric iron in CaSiO_3 perovskite at high pressure

ZHONGWU WANG^{1,2} AND T. YAGI¹

1. Institute for Solid State Physics, The University of Tokyo, Roppongi, Tokyo 106, Japan

2. GEMOC, School of Earth Sciences, Macquarie University, Sydney 2109, Australia

ABSTRACT

Synthetic andradite ($\text{Ca}_3\text{Fe}_2\text{Si}_3\text{O}_{12}$) has been compressed to loading pressures >21 GPa and heated to $\sim 1000^\circ\text{C}$ by a YAG laser in a Diamond Anvil Cell (DAC). After quenching to room temperature, X-ray diffraction of the sample, still held at 21 GPa, showed that andradite had transformed to a cubic perovskite type polymorph with $a = 3.460(4)$ Å. Upon decompression the perovskite phase transformed into an amorphous phase. The density of the perovskite polymorph ($\text{Ca}_3\text{Fe}_2\text{Si}_3\text{O}_{12}$) is $\sim 13.6\%$ greater than that of isochemical andradite at 21 GPa. Ferric iron replaces Ca^{2+} and Si^{4+} in the perovskite structure ($\text{Fe}^{3+} + \text{Fe}^{3+} = \text{Si}^{4+} + \text{Ca}^{2+}$), giving a formula unit: $(\text{Ca},\text{Fe}^{3+})(\text{Si},\text{Fe}^{3+})\text{O}_3$. The new Fe^{3+} -rich Ca-perovskite may provide new insight into the controls on the electrical conductivity of the lower mantle.

KEYWORDS: andradite, high pressure, X-ray diffraction, perovskite, lower mantle.

Introduction

BECAUSE of the special significance of ferric iron for the geophysics of solid earth interior, the presence of ferric iron in mantle minerals is of particular current interest. Evidence from *in situ* high-pressure Mössbauer spectra and from the components of diamond inclusions derived from the lower mantle shows that ferric iron can be incorporated into perovskite $(\text{Mg},\text{Fe})\text{SiO}_3$ and magnesio-wüstite $(\text{Fe},\text{Mg})\text{O}$ (Harris *et al.*, 1997; McCammon *et al.*, 1997). We have studied andradite ($\text{Ca}_3\text{Fe}_2\text{Si}_3\text{O}_{12}$) by high-pressure X-ray diffraction to explore its stability at mantle conditions and to obtain a deeper understanding of the structural aspects of its high-pressure phase transitions, in the context of the geophysical properties of the Earth's interior. In this letter, the results of these high-pressure X-ray diffraction investigations are presented and discussed.

Experimental

High-pressure synthesis of andradite

CaCO_3 , Fe_2O_3 and SiO_2 were mixed in a molar ratio of 3:1:3 and ground in a ceramic mortar. The

initial mixture was held at 1000°C for 24 h to decarbonate the CaCO_3 . Thus, a starting material was obtained with a bulk composition near stoichiometric $\text{Ca}_3\text{Fe}_2\text{Si}_3\text{O}_{12}$, which was used for subsequent high-pressure synthesis.

High-pressure runs were carried out using a wedge-type cubic anvil apparatus (Hishinuma and Yagi, 1994). Temperatures were measured using a Pt-Pt13%Rh thermocouple. The pure andradite was formed at 1150°C and 3 GPa in 1 h runs. The unit-cell parameter was determined by conventional X-ray powder diffraction (monochromatic $\text{Cr-K}\alpha_1$ radiation) from at least 10 peaks at $>100^\circ 2\theta$. The lattice parameter of the synthetic andradite was $a = 12.068(2)$ Å (Ia3d), in good agreement with the pioneering results of Woodland and O'Neill (1995).

In situ high-pressure X-ray diffraction

High-pressure X-ray diffraction measurements were carried out at the synchrotron radiation source at the High Energy Physics Institute (KEK) using a modified Mao-Bell type Diamond Anvil Cell (DAC). The diamond culet was 450 μm in diameter. The powder sample was squeezed

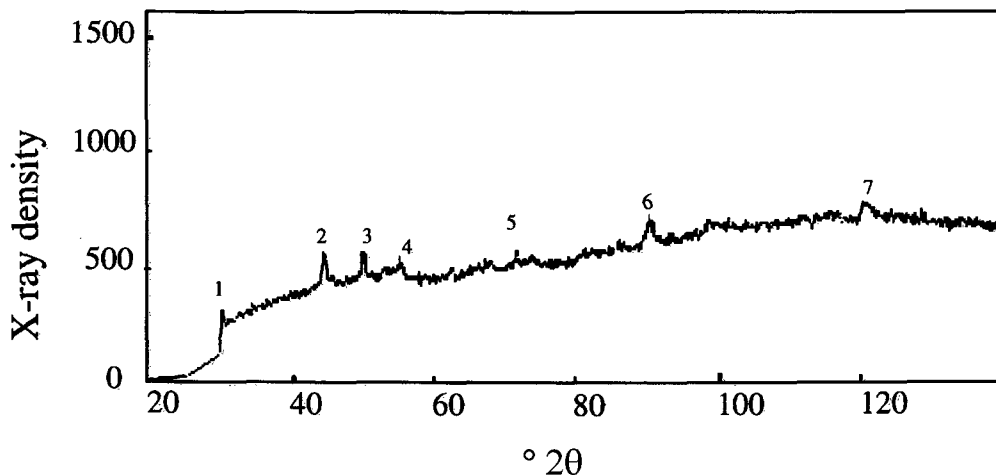


FIG. 1. Room temperature and pressure X-ray diffraction pattern of a sample recovered from a high- P/T run (26.9 GPa with laser heating). The seven weak peaks indicated are attributed to andradite.

between two diamond anvils and compacted into a disk (150 μm in diameter and 10 μm thick) in a stainless steel gasket.

The pressure was calibrated using the R_1 fluorescence of ruby (Mao *et al.*, 1978). After the fine powdered sample had been compressed to 20–30 GPa in the DAC, it was heated to $\sim 1000^\circ\text{C}$ using a YAG laser. This process was carried out for 2 h to make sure the sample was heated sufficiently. The recovered sample, retained at high pressure within the DAC, was observed by optical microscopy and then examined by X-ray diffraction to identify the phases present under temperature-quenched conditions. Furthermore, monochromatic synchrotron radiation ($\lambda = 0.4313 \text{ \AA}$, $2\theta = 5\text{--}25^\circ$) was employed to chart any structural changes upon release of pressure.

Results and discussion

In situ high-pressure optical observation revealed that, before laser heating, the sample was transparent, while after laser heating it had become optically opaque. The change in colour was the first important indicator of the existence of a possible phase transformation. X-ray diffraction on the recovered sample at 0 GPa showed that andradite had transformed into an amorphous phase, showing several weak diffraction peaks upon a high background (Fig. 1).

The X-ray diffraction patterns obtained from the temperature-quenched sample at 1 atmosphere and 21 GPa are shown in Fig. 2. Eight intense

lines in the high-pressure diffraction pattern could not be attributed to andradite. The positions of these peaks are similar to those of CaSiO_3 perovskite (Liu and Ringwood, 1975; Yagi *et al.*, 1989), and all of them can readily be indexed in terms of the cubic perovskite structure (Table 1). At 21 GPa, the new phase of $\text{Ca}_3\text{Fe}_2\text{Si}_3\text{O}_{12}$ shows some very strong peaks, and upon decompression this new phase was retained, but as the pressure approached 0 GPa its diffraction signal disappeared as it transformed into an amorphous phase. It is worth pointing out that andradite peaks are present in all patterns, coexisting with the cubic phase due to incomplete transformation.

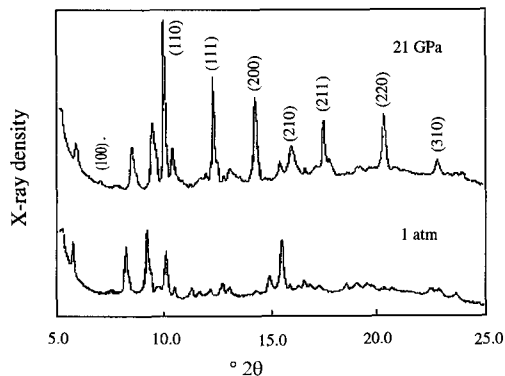


FIG. 2. X-ray diffraction patterns of $\text{Ca}_3\text{Fe}_2\text{Si}_3\text{O}_{12}$ at pressures of 1 atmosphere and 21 GPa. Indexed peaks refer to the cubic perovskite structure.

TABLE 1. The Bragg positions of Ca-Fe-perovskite obtained *in situ* in a diamond-anvil high-pressure camera at 21 GPa

<i>hkl</i>	<i>d</i> _(obs) (Å)	<i>d</i> _(cal) (Å)	<i>d</i> _(o) / <i>d</i> _(c) - 1
100	3.468	3.460	0.002
110	2.462	2.447	0.006
111	1.995	1.998	-0.001
200	1.731	1.730	0.001
210	1.544	1.547	-0.002
211	1.422	1.413	0.007
220	1.223	1.223	-0.001
310	1.092	1.094	-0.002

TABLE 2. Pressure dependence of the unit cell volume of perovskite (Ca,Fe)(Si,Fe)O₃ at room temperature

Pressure (GPa)	Unit cell volume (Å ³)
21	41.42
17	42.39
13	43.38
10	44.01

* *a* = 3.460 (4)Å and *V* = 41.42 (14)Å³

The cubic cell parameter was determined as a function of pressure on decompression (Table 2). Comparison of the compressibility of the cubic Ca₃Fe₂Si₃O₁₂ phase with that of CaSiO₃ perovskite (Tamai and Yagi, 1989; Yagi *et al.*, 1989; see Fig. 3) shows that, at pressures >20 GPa, the unit cell is noticeably smaller than that of CaSiO₃

perovskite, but with decreasing pressure its cell volume becomes gradually closer to that of CaSiO₃ perovskite. At ~11 GPa the cell volumes are almost equal, and below this pressure the cell volume of the new perovskite phase is greater than that of Ca-perovskite. Considering the ionic radii of Si⁴⁺, Fe³⁺ (Fe³⁺ > Si⁴⁺) and Ca²⁺ (Fe³⁺ < Ca²⁺), and taking account of charge balance, it is reasonable to suggest that this new high-pressure phase can be written as (Ca,Fe)(Si,Fe)O₃, with ferric iron replacing Ca²⁺ and Si⁴⁺ in the CaSiO₃ perovskite structure (Fe³⁺ + Fe³⁺ = Si⁴⁺ + Ca²⁺).

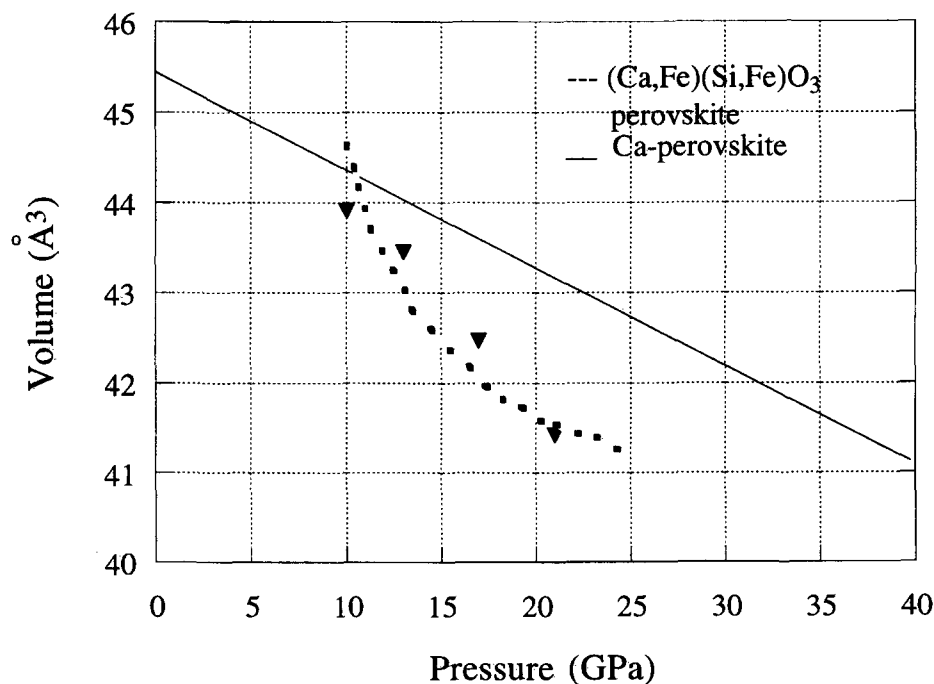


FIG. 3. Compressibilities of CaSiO₃ perovskite (after Tamai and Yagi, 1989) and (Ca,Fe)(Si,Fe)O₃ perovskite (this study; triangles).

The lattice parameter is calculated to be 3.460(4) Å at 21 GPa and room temperature. This yields a density of 5.09 g/cm³, which is ~13.6% greater than that of an isochemical andradite at the same pressure.

The diffraction pattern of (Ca,Fe)(Si,Fe)O₃ perovskite was followed upon release of pressure. Some runs were conducted at about 20 GPa and 30 GPa, and in all cases the recovered materials consisted of glass with a few weak lines corresponding to the andradite, which is present due to incomplete transformation. The zero-pressure lattice parameter of the perovskite modification of (Ca,Fe)(Si,Fe)SiO₃ was not measurable experimentally. Extrapolation of lattice parameters from (Ca,Fe)(Si,Fe)SiO₃ obtained at different pressures gives a higher value than that of Ca-perovskite (CaSiO₃) (Fig. 3). Because there was no pressure-transmitting medium present, pressure gradients must exist in the sample. Taking these gradients into account, and noting the difference in colour of andradite and the perovskite phase, the transformation pressure for andradite to perovskite is estimated at ~15–17 GPa. Based on previous data and our results on CaSiO₃–Fe₂O₃, an increase in ferric iron content may increase this transition pressure under isothermal conditions (Fig. 4). However, further studies on the CaSiO₃–Fe₂O₃ system will have to be carried out to clarify the position of the phase boundary and the stability field for Fe³⁺-bearing perovskite.

A series of studies on diamond inclusions derived from the deeper mantle have indicated that ferric iron can enter perovskite (Fe,Mg)SiO₃ and magnesiowüstite (Mg,Fe)O (McCammon *et al.*, 1997; Harris *et al.*, 1997; McCammon, 1997), and that the concentration of ferric iron is (positively) correlated to Al₂O₃-content. Our high-pressure experiments provide further very strong evidence that Fe³⁺ can be incorporated into Ca-perovskite in the lower mantle. Previous electrical conductivity measurements on the lower mantle minerals magnesiowüstite and perovskite (Li and Jeanloz, 1990; Poirier and Peyronneau, 1992) provide conflicting results. The ambient temperature electrical conductivity of perovskite and a mixture of (Mg,Fe)SiO₃ perovskite and (Mg,Fe)O magnesiowüstite, measured by Li and Jeanloz (1990) is lower, by about three orders of magnitude, than that reported by Poirier and Peyronneau (1992). The results of Poirier and Peyronneau, extrapolated to lower mantle pressures, are in agreement with the

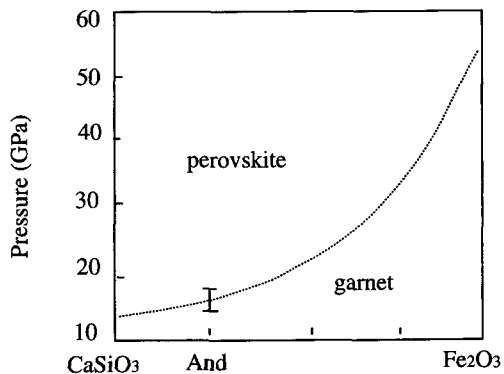


FIG. 4. Possible pressure-composition phase diagram for the garnet-perovskite transition (And: andradite).

value of 1 S/m at a depth of 1000 km, determined from the analysis of the transient and secular variations of geomagnetic field. In light of this result, it is of interest that Poirier and Peyronneau (1992) suggested a conduction mechanism in perovskite that involves electronic charge transfer between Fe²⁺ and Fe³⁺ to explain their high electrical conductivity. Based on the above data and conductivity mechanisms in semiconductors, it is both necessary and reasonable to deduce that another more highly conductive and interconnected phase exists in lower mantle (Li and Jeanloz, 1993). Thus, either Fe³⁺ doping in mantle minerals or the presence of a new Fe³⁺-bearing perovskite phase could play an important role in the control of geophysical parameters, bearing in mind that the doping in semiconductors can induce huge increases in electrical conductivity. Although <10% Ca-perovskite can enter a lower mantle of pyrolite composition, Fe³⁺-rich Ca-perovskite might still provide an important control on geophysical evolution of lower mantle (just as, e.g. 4–5 wt.% Al₂O₃ could: Wood and Rubie, 1996). There is no doubt that the presence of ferric iron can significantly affect the geochemical and geophysical properties of lower mantle, including its density and electrical conductivity.

In conclusion, we have demonstrated the existence of a perovskite type modification of Ca₃Fe₂Si₃O₁₂ at high pressures, which supports the existence of ferric iron in the lower mantle, based on mantle xenoliths. As suggested elsewhere, it seems probable that (Ca,Fe)(Si,Fe)SiO₃ perovskite is a significant constituent of the lower mantle, especially considering the electrical

conductivity of mantle mineral mixtures. In the light of these discoveries, it seems likely that the mineral species of the lower mantle possess more abundant ferric iron than ferrous iron.

Acknowledgements

We acknowledge financial support from the Ministry of Sciences, Technology and Education of Japan and from the GEMOC Key Centre to Z. Wang. We thank S.Y. O'Reilly and W.L. Griffin for many useful discussions. The manuscript was improved by a critical review from Dr Simon Redfern, for which we are grateful. This is publication number 118 in the ARC National Key Centre for the Geochemical Evolution and Metallogeny of Continents.

References

- Harris, J., Hutchison, M.T., Hursthouse, M., Light, M. and Harte, B. (1997) A new tetragonal silicate mineral occurring as inclusions in lower mantle diamonds. *Nature*, **387**, 486–9.
- Hishinuma, T. and Yagi, T. (1994) Surface tension of iron hydride formed by the reaction of iron silicate water under pressure. *Proc. Japan Acad.*, **70**, Ser B, 71–6.
- Li, X. and Jeanloz, R.L. (1990) Laboratory studies of the electrical conductivity of silicate perovskite at high pressure and high temperature. *J. Geophys. Res.*, **95**, 5067–87.
- Liu, L-G. and Ringwood, A.E. (1975) Synthesis of a perovskite type polymorph of CaSiO₃. *Earth Plan. Sci. Lett.*, **28**, 209–11.
- Mao, H.K., Bell, P.M., Shaner, J.W. and Steinberg, D.J. (1978) Specific volume measurements of Cu, Mo, Pd, and Ag calibration of the ruby R₁ fluorescence pressure gauge from 0.05 to 1 Mbar. *J. Appl. Phys.*, **49**, 3276–87.
- McCammon, C. (1997) Perovskite as a possible sink for ferric iron in the lower mantle. *Nature*, **387**, 694–6.
- McCammon, C., Hutchinson, M. and Harris, J.W. (1997) Ferric iron content of mineral inclusions in diamonds from Sao Luiz: A view into the lower mantle. *Science*, **278**, 434–6.
- Poirier, J.B. and Peyronneau, J. (1992) Experimental determination of the electrical conductivity of the material of the Earth's lower mantle. In *High pressure research in mineral Physics: Application to Earth and Planetary Sciences*, (Y. Syono and M.H. Maghni, eds.), **77–78**, Tena Scientific Tokyo.
- Tamai, H. and Yagi, T. (1989) High pressure and high temperature phase relations in CaSiO₃ and CaMgSi₂O₆ and elasticity of perovskite-type CaSiO₃. *Phys. Earth Planet. Inters.*, **54**, 370–7.
- Wood, B.J. and Rubie, D.C. (1996) The Effect of Alumina on phase transformations at the 660-kilometre discontinuity from Fe-Mg partitioning experiments. *Science*, **273**, 1522–4.
- Woodland, A.B. and O'Neill, H.St.C. (1995) Phase relation between Ca₃Fe³⁺Si₃O₁₂ -Fe²⁺₃Fe³⁺₂Si₃O₁₂ garnet and CaFeSi₂O₆ pyroxene solid solutions. *Contrib. Mineral. Petrol.*, **121**, 7–98.
- Yagi, T., Kusanagi, S., Tsuchida, Y. and Fukai, Y. (1989) Isothermal compression and stability of perovskite-type CaSiO₃. *Proc. Japan Acad.*, **65**, Ser. B, 129–32.

[Manuscript received 29 April 1998:
revised 23 June 1998]